Astron. Astrophys. 338, 592–598 (1998)

ASTRONOMY
AND
ASTROPHYSICS

Monitoring of dust-enshrouded AGB stars in the LMC

P.R. Wood

Mount Stromlo and Siding Spring Observatories, Private Bag, Weston Creek PO, ACT 2611, Australia (wood@mso.anu.edu.au)

Received 16 March 1998 / Accepted 3 July 1998

Abstract. Twelve IRAS sources in the LMC with colours similar to those expected for dust-enshrounded AGB stars have been monitored in the infrared for 1880 days. The objects come from the list of Reid (1991). Nine of these objects are large amplitude variables with periods in the range 530 to 1295 days. The variability confirms their status as dust-enshrouded AGB stars. Combined with the results of Wood et al. (1992), a total of 15 large amplitude, dust-enshrouded AGB stars are now known in the LMC but it is estimated that many hundreds more await discovery. The objects studied in this paper are $\sim$2 magnitudes fainter in $M_{\rm bol}$ than the previously known variables. The low luminosities of six of the new objects suggest that they are evolving from the tip of the AGB of the dominant intermediate-age LMC population which has an initial mass $\sim$1.5$M_{\odot}$ and age $\sim$2-3$\times10^9$ years. It is suggested that these stars should be carbon-rich although several of them have been tentatively classified as oxygen-rich. The period range of the objects is consistent with that expected from theoretical models of AGB evolution with mass loss. The observations presented here clearly demonstrate that once significant mass loss and dust formation occurs, large amplitude LPVs no longer fall on the tight ($M_{\rm bol}$, $\log P$) or (K, $\log P$) relation found for the Mira variables with $P \lesssim 450$ days.

Key words: stars: AGB – stars: late-type – stars: variables: other – Magellanic Clouds – infrared: stars

1. Introduction

During the final stages of AGB evolution, stars develop large amplitude, long period pulsations, undergo rapid mass loss, and become enveloped in a dense shell of dust and gas. In the early phases of this process, the AGB stars are visible as Mira variables while in the latter stages they are pulsating infrared sources. If they are oxygen-rich, they will be OH/IR stars.

The quantitative understanding of the properties of stars in the final evolutionary stages is greatly helped if accurate distances, and hence luminosities, can be derived. This has led to a large effort to detect long-period variables (LPVs) in the Magellanic Clouds where the distance and foreground reddening are well known. In the LMC in recent times, Wood et al. (1985), Glass & Reid (1985), Reid et al. (1988), Hughes(1989) and Reid et al. (1995) have used time series of I Schmidt plates to determine periods for LPVs without thick dust shells. The combination of derived periods with infrared JHK photometry (Wood et al. 1983; Hughes & Wood 1990; Feast et al. 1989) has led to a clear picture of the properties (masses, luminosities, period-luminosity relations) for the optically-visible LPVs.

Such a clear picture is not yet available for stars in the very latest stages of AGB evolution. These stars are not readily detectable in the optical bands due to their thick surrounding dust shells which emit the star's energy mostly in the infrared. The IRAS satellite provided a means of detecting the more luminous of these shells over a wide area of the LMC. Schwering (1988) and Reid et al. (1990) utilized all the IRAS data to form deep catalogs of point sources in the LMC. Reid (1991), Zijlstra et al. (1996), van Loon et al. (1997, 1998) and Loup et al. (1997) have subsequently selected point sources from these catalogs with colours similar to those expected for dust-enshrouded AGB stars and published single phase, ground-based, near infrared magnitudes. In this paper, monitoring of a selection of objects detected by Reid (1991) is reported. The monitoring provides accurate mean magnitudes and periods, both quantities being needed for a proper understanding of the latest stages of AGB evolution.

2. Observations and data reduction

The observations were made over 1880 days from August 1992 to October 1997 on the 2.3m telescope at Siding Spring Observatory. Prior to March 1994, the observations were made with a single channel infrared photometer while more recent observations were made with the near infrared array camera CASPIR (McGregor et al. 1994). For the CASPIR data, the images were bias-subtracted, linearized and flatfielded using the IRAF data reduction package. Photometry of each frame was obtained by running the IRAF task QPHOT. The single channel $JHKL$ photometry was converted to the AAO $JHKL'$ system using the transforms of McGregor & Hyland (1981). The CASPIR photometry was also converted to the AAO system using the transforms in McGregor (1994) for JHK and Wood et al. (1998) for L'. Individual $JHKL'$ measurements are given in Table 1. The formal errors in the photometry are typically

Send offprint requests to: P.R. Wood

Table 1. Infrared photometry of the TRM sources

$JD244$	J	H	K	L'	$JD244$	J	H	K	L'	$JD244$	J	H	K	L'
TRM4					9852	-	15.71	13.02	-	9500	15.00	12.88	10.94	8.45
8851	-	-	11.82	-	9945	-	-	12.95	-	9559	14.86	-	10.91	8.30
8932	-	15.14	12.06	8.74	10059	-	-	11.92	-	9641	-	-	11.14	-
8993	-	-	12.62	-	10121	-	-	11.75	-	9706	-	-	11.67	-
9261	-	-	13.17	-	10350	-	-	12.12	-	9768	-	-	12.37	-
9318	-	-	12.97	9.42	10529	-	-	13.21	-	9830	-	-	12.38	-
9374	-	15.04	12.58	9.37	10731	-	-	12.11	-	9852	16.56	14.39	12.29	9.37
9437	-	14.90	12.06	8.83	TRM45					9945	-	-	12.04	-
9500	17.17	14.43	11.84	8.29	8932	15.88	12.98	10.97	8.81	10059	-	-	11.29	-
9559	17.12	-	11.74	8.17	8993	15.46	13.22	11.07	-	10121	-	-	11.22	-
9641	-	-	11.68	-	9261	15.91	13.32	11.23	9.20	10350	-	-	12.44	-
9706	-	-	11.80	-	9317	15.82	12.85	10.80	8.75	10529	-	-	11.83	-
9768	-	-	12.24	-	9375	-	12.56	10.64	8.69	10731	-	-	10.84	-
9830	-	-	12.54	-	9437	15.37	12.94	10.76	8.48	TRM77				
9852	-	15.85	12.70	-	9500	15.47	12.86	10.77	8.69	8851	-	-	12.79	-
9945	-	-	13.36	-	9559	15.94	-	11.14	8.69	8932	-	-	13.35	9.36
10059	-	-	13.11	-	9641	-	-	11.51	-	8993	-	-	13.46	9.58
10350	-	-	11.69	-	9706	-	-	11.66	-	9259	-	15.15	12.42	9.40
10529	-	-	11.76	-	9768	-	-	11.61	-	9261	-	-	12.50	-
10731	-	-	12.94	-	9830	-	-	11.04	-	9317	-	15.08	12.54	9.60
TRM20					9852	15.48	12.89	10.82	8.62	9374	-	-	12.68	-
8851	-	-	12.60	-	9945	-	-	10.52	-	9437	-	-	13.42	-
8932	-	15.51	12.17	8.70	10059	-	-	10.71	-	9500	-	-	13.79	9.49
8993	-	-	12.03	-	10350	-	-	11.30	-	9559	-	-	13.83	9.99
9261	-	-	12.90	9.20	10529	-	-	10.57	-	9641	-	-	13.06	-
9317	-	-	13.19	-	10731	-	-	11.44	-	9706	-	-	12.56	-
9374	-	-	13.26	-	TRM60					9768	-	-	12.49	-
9437	-	-	13.57	9.38	8851	-	-	10.58	-	9830	-	-	12.39	-
9499	-	-	13.90	9.45	8932	-	13.35	10.72	8.45	9852	-	15.12	12.49	9.05
9559	-	-	14.02	9.57	8993	-	13.34	10.74	8.42	9945	-	-	13.03	-
9641	-	-	13.43	-	9261	15.93	12.24	9.70	7.41	10059	-	-	13.66	-
9706	-	-	12.83	-	9317	15.91	11.87	9.48	7.16	10350	-	-	12.28	-
9768	-	-	12.37	-	9375	-	11.65	9.35	6.95	10529	-	-	13.25	-
9830	-	-	12.22	-	9437	15.40	11.79	9.22	6.77	10731	-	-	12.69	-
9852	-	15.54	12.09	8.29	9500	15.05	11.50	9.16	6.54	TRM79				
9945	-	-	12.18	-	9559	15.08	-	9.14	6.63	8851	-	-	11.68	-
10059	-	-	12.10	-	9641	-	-	9.15	-	8932	-	13.96	11.53	8.71
10350	-	-	13.35	-	9706	-	-	9.30	-	8993	-	13.84	11.50	8.65
10529	-	-	13.61	-	9768	-	-	9.61	-	9261	-	15.72	12.84	9.88
10731	-	-	12.25	-	9830	-	-	9.76	-	9317	-	-	13.06	-
TRM24					9852	15.60	12.19	9.85	7.42	9374	-	-	13.07	-
8851	-	-	11.71	-	9945	-	-	10.12	-	9437	-	-	12.94	9.17
8932	16.29	14.64	12.14	9.00	10059	-	-	10.34	-	9500	-	14.81	12.11	8.80
8993	16.81	15.11	12.70	-	10350	-	-	10.85	-	9559	17.38	-	11.84	8.53
9261	-	14.78	12.92	9.58	10529	-	-	9.72	-	9641	-	-	11.53	-
9318	-	-	12.50	9.37	10731	-	-	9.25	-	9706	-	-	11.47	-
9374	-	14.25	11.78	8.65	TRM72					9768	-	-	11.95	-
9437	-	14.25	11.59	8.31	8851	-	-	10.99	-	9830	-	-	12.27	-
9499	16.71	14.05	11.41	8.12	8932	14.81	12.45	10.56	8.44	9852	-	15.46	12.47	8.72
9559	16.81	-	11.68	8.34	8993	14.65	12.33	10.42	8.35	9945	-	-	13.02	-
9641	-	-	12.06	-	9259	-	13.76	11.78	9.20	10059	-	-	13.14	-
9706	-	-	12.64	-	9317	15.75	13.51	11.67	9.22	10350	-	-	11.80	-
9768	-	-	13.16	-	9375	-	13.45	11.54	9.02	10529	-	-	12.37	-
9830	-	-	13.16	-	9437	15.44	-	11.50	9.01	10731	-	-	13.33	-

Notes. JD244 is Julian Date - 2440000. The TRM numbers are those given by Reid et al. (1990).

Table 1. (continued)

$JD244$	J	H	K	L'	$JD244$	J	H	K	L'	$JD244$	J	H	K	L'
TRM88					10350	-	-	9.53	-	10059	-	-	8.81	-
8851	-	-	10.77	-	10529	-	-	9.88	-	10350	-	-	9.22	-
8932	15.19	13.18	11.21	9.46	10731	-	-	10.20	-	10529	-	-	8.99	-
8993	-	13.32	11.42	-	TRM101					10731	-	-	8.77	-
9261	14.25	12.30	10.36	8.41	8851	-	-	8.84	-	TRM108				
9317	14.30	12.08	10.38	8.39	8932	9.81	9.11	8.66	7.70	8932	9.10	8.16	7.79	7.34
9375	14.76	12.20	10.43	8.24	8993	9.85	9.22	8.75	-	8993	9.10	8.14	7.80	7.26
9437	14.75	12.59	10.70	8.21	9259	9.79	9.11	8.55	7.70	9317	9.27	8.23	7.91	7.43
9501	-	-	10.83	-	9317	9.77	9.04	8.58	7.71	9375	9.25	8.21	7.90	7.45
9559	14.77	-	10.86	8.61	9375	9.89	9.14	8.68	7.72	9768	-	-	7.90	-
9641	-	-	10.55	-	9437	10.06	9.31	8.76	7.83	TRM129				
9706	-	-	10.38	-	9501	-	-	8.89	-	8851	-	-	7.83	-
9768	-	-	10.10	-	9559	10.27	-	8.85	7.90	8932	9.24	8.14	7.74	7.10
9830	-	-	9.80	-	9641	-	-	8.75	-	8993	9.29	8.20	7.70	7.14
9852	13.11	11.21	9.77	8.11	9768	-	-	8.76	-	9317	9.31	8.19	7.75	7.09
9945	-	-	9.85	-	9830	-	-	8.79	-	9375	9.33	8.24	7.78	7.14
10059	-	-	10.23	-	9852	-	-	8.81	-	9436	-	-	7.77	-
10121	-	-	10.27	-	9945	-	-	8.81	-	9768	-	-	7.83	-

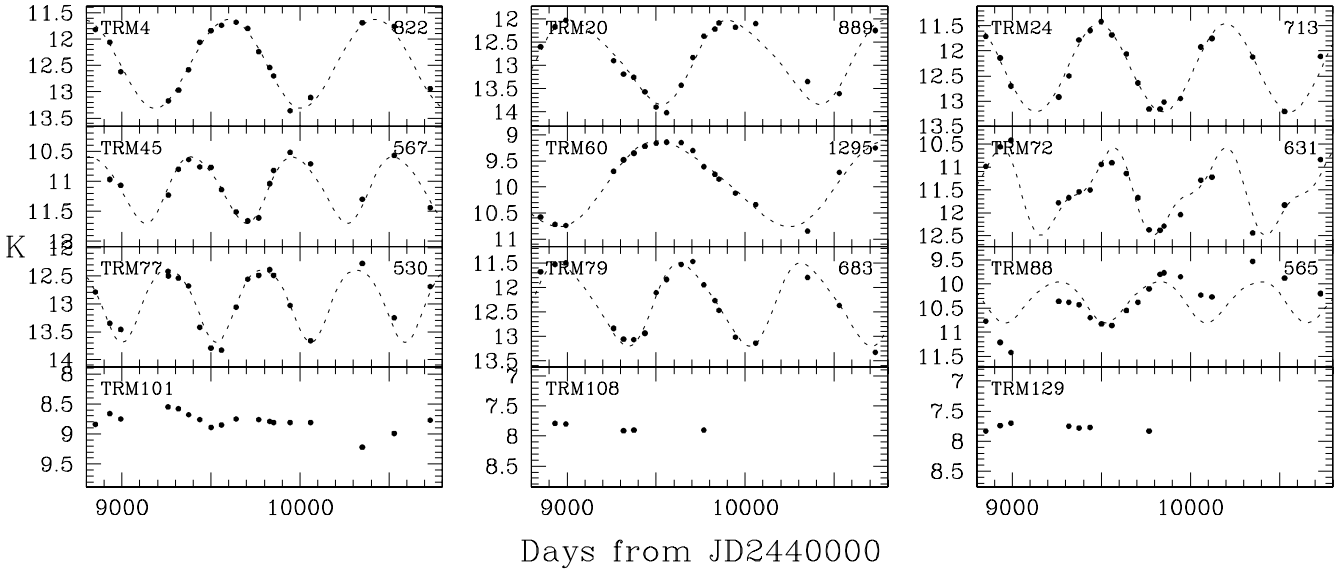

Fig. 1. K light curves of the monitored sources (dots). The dashed curve is the Fourier fit to the light curve described in the text. The TRM number of each source and the adopted period (in days) from Table 2 is shown on each panel.

less than 0.15, 0.1, 0.05 and 0.15 magnitudes for J, H, K and L', respectively.

3. Period determinations and mean properties

The K light curves of the sources are shown in Fig. 1. It is clear that the first 9 sources show large amplitude, periodic variations. In the case of TRM 88, there is both a variation with a period of $\sim$550 days and a long term brightening. The last three sources (TRM 101, 108 and 129) are much brighter than the other sources and they show no, or only small amplitude, variability. All three are known M stars (Loup et al. 1997). Their spectral types, small amplitude of variability and bolometric luminosities (Table 2) are consistent with them being LMC red supergiants (e.g. Wood et al. 1983), where red supergiants are defined as stars more massive than the upper mass limit for AGB stars ($\sim$8 $M_{\odot}$).

Periods were determined for the large amplitude variables using the phase dispersion minimization (PDM) method of Stellingwerf (1978). In order to derive flux-mean K magnitudes for the variables, some of which have K amplitudes near 2 magnitudes, a least-squares Fourier fit (consisting of the fundamental period and first harmonic) was made to each light curve using the period obtained from PDM. The resultant light curve fits are shown as dashed lines on Fig. 1. The flux-mean $<K>$

magnitudes were derived by integrating the instantaneous flux obtained from the Fourier fits.

The properties of the TRM objects are summarized in Table 2. In this table, TRM is the identification number of Reid et al. (1990), RA and Dec are the right ascension and declination (epoch 1950), $<K>$ is the flux-mean K magnitude derived from the Fourier fit to the light curve, P is the period in days and ΔK is the full amplitude of the K light variations given by the Fourier fit. The colours $<J-K>$, $<H-K>$ and $<K-L'>$ are simple averages of the observed values. The fluxes $S12$ and $S25$ (Jy) at 12 and 25 μm, respectively, given in Table 2 are estimated at mean light. They were derived by adopting mid-August 1983 (JD2445550) as the mean date of the IRAS observations, then assuming that the light curve amplitude at 12 and 25 μm was 0.8 times as large as at K. This ratio came from inspection of the multiwavelength light curves of dusty AGB stars published by Harvey et al. (1974) and Le Bertre (1993).

Absolute bolometric luminosities for each star were calculated by integrating under the mean flux curve of each object as described in Wood et al. (1992). A distance modulus to the LMC of 18.50 was assumed. Errors in $M_{\rm bol}$ come from a number of sources. An examination of the flux distributions of the large amplitude variables (the first 9 sources in Table 2) shows that most of the energy flux is emitted near the L', 12 μm and K bands, in order of decreasing importance. The error in the mean K flux estimate is very small as it is obtained from many K measures, each of which has an error less than 0.05 magnitudes. The mean L' magnitude is derived from the mean K magnitude and the mean $<K-L'>$ colour. The main source of error in L' is the error in $<K-L'>$. This latter error is dominated by the small number of measures (typically 7) of $<K-L'>$, which typically varies with a semi-amplitude of 0.4 magnitudes. Assuming random sampling, the error in $<K-L'>$ is thus $\sim 0.4/\sqrt{7} \approx 0.15$ magnitudes. Thus, given the small uncertainty in $<K>$, the error in $<L'>$ is also $\sim$0.15 magnitudes (note that this error dominates the error in $<L'>$ resulting from the individual photometric errors of 0.15 magnitudes: for 7 measures, the photometric error in $<L'>$ is $\sim 0.15/\sqrt{7} \approx 0.06$ mag.). The measurement error in the 12 μm flux is probably about 10% (Schwering 1988). Another source of error at 12 μm lies in the assumed amplitude of the 12 μm light curve. Although the ratio of 12 μm amplitude to K amplitude has been assumed to be 0.8, values from $\sim$0.6–1.0 occur in the examples of Harvey et al. (1974) and Le Bertre (1993). Assuming an error of 0.2 in the amplitude ratio, an average K semi-amplitude of 0.75 magnitudes, and that the phase of measurement is at maximum or minimum light where the amplitude error will be have the largest impact, an error in 12 μm flux of 0.2$\times$0.75=0.15 magnitudes will result. Overall then, there is a negligible error in $<K>$, and errors close to 0.15 magnitudes in the $<L'>$ and mean 12 μm fluxes. The error in the derived $M_{\rm bol}$ is therefore expected to be approximately 0.15 magnitudes.

There are two objects in common between the present study and that of Wood et al. (1992), TRM 60 = IRAS 05329-6708 and TRM 129 = IRAS 05261-6614. The object TRM 129 is a small amplitude variable and the $M_{\rm bol}$ value derived here (-7.65) is similar to that derived by Wood et al. (-7.52). For TRM 60, the period derived here (1295 days) is in good agreement with the Wood et al. value (1260 days). However, the $M_{\rm bol}$ derived here (-6.43) is significantly fainter than the value derived by Wood et al. (-6.86) because of the phase correction to the IRAS fluxes used here (TRM 60 was observed near maximum light by IRAS). In the rest of this paper, we use the currently derived properties for TRM60.

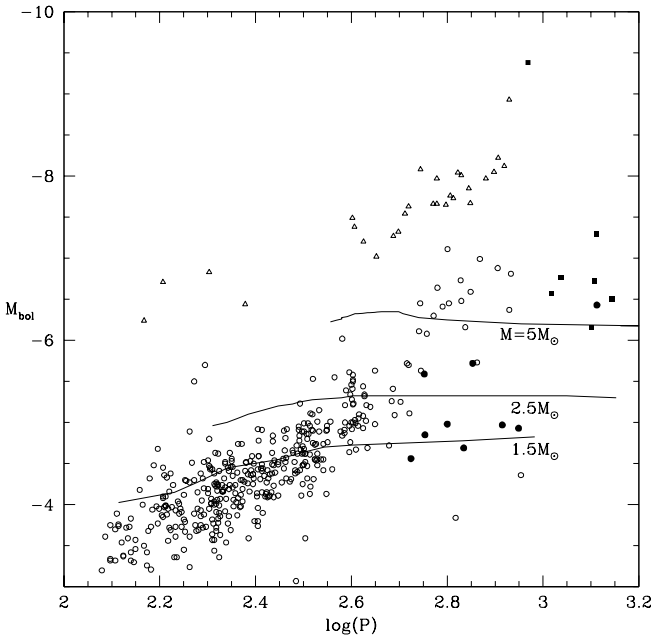

Fig. 2. The $(M_{\rm bol}, \log P)$ diagram for LPVs in the LMC. The TRM sources studied here are shown as filled circles, the IRAS sources studied by Wood et al. (1992) are shown as filled squares, optically-visible LMC LPVs from Hughes & Wood (1990) are shown as open circles while supergiants from Wood et al. (1983) are shown as open triangles. The lines show mean evolutionary tracks (excluding excursions at helium shell flashes) from Vassiliadis & Wood (1993). Evolution is towards longer periods.

4. Discussion

4.1. Evolutionary status of the observed TRM sources

The TRM sources are shown in the $(M_{\rm bol}, \log P)$ diagram, Fig. 2, as filled circles. Periods and luminosities have previously been determined for a group of similar, but more luminous, dusty LMC IRAS sources by Wood et al. (1992) and these are shown as filled squares in Fig. 2. The position occupied by optically-visible LPVs on the AGB in the LMC is illustrated by the open circles (from Hughes & Wood 1990) while the triangles show the position occupied by supergiants in the LMC (Wood et al. 1983). Finally, the lines show the evolutionary tracks of 1.5, 2.5 and 5 $M_{\odot}$ LMC stars during the optically-visible and superwind phases of AGB evolution according to the models of Vassiliadis & Wood (1993).

It is clear from Fig. 2 that the TRM and IRAS sources have much longer periods at a given luminosity than the optically-

Table 2. Properties of the TRM sources

TRM	RA	Dec	$<K>$	$<J-K>$	$<H-K>$	$<K-L'>$	$S12$	$S25$	$M_{\rm bol}$	P	ΔK
4	5 11 17.8	-67 55 43	12.29	5.36	2.82	3.40	0.17	0.12	-4.97	822	1.69
20	5 19 03.6	-67 48 02	12.72	-	3.39	4.01	0.14	0.09	-4.93	889	1.81
24	5 11 19.0	-67 39 44	12.17	4.67	2.46	3.24	0.51	0.30	-5.72	713	1.75
45	5 28 20.6	-67 22 37	11.04	4.72	2.07	2.15	0.09	-	-4.85	567	1.10
60	5 32 55.1	-67 08 53	9.77	6.07	2.46	2.40	0.36	0.69	-6.43	1295	1.65
72	5 11 38.0	-66 54 41	11.39	4.11	1.94	2.47	0.15	0.10	-4.98	631	1.90
77	5 36 02.6	-66 48 24	12.87	-	2.63	3.63	0.11	0.09	-4.56	530	1.29
79	5 30 05.1	-66 51 38	12.17	5.54	2.67	3.25	0.09	0.07	-4.69	683	1.70
88	5 20 18.0	-66 38 44	10.30	3.92	1.80	2.04	0.19	-	-5.59	565	0.85
101	5 31 43.3	-66 05 43	8.77	1.23	0.49	0.92	0.36	0.35	-7.00	-	-
108	5 23 36.1	-65 44 38	7.86	1.33	0.33	0.48	0.32	0.18	-7.67	-	-
129	5 26 07.6	-66 14 37	7.77	1.55	0.45	0.62	0.31	0.23	-7.65	-	-

Note. The right ascension and declination (equinox 1950) were obtained from the telescope coordinates and should be accurate to $2''$.

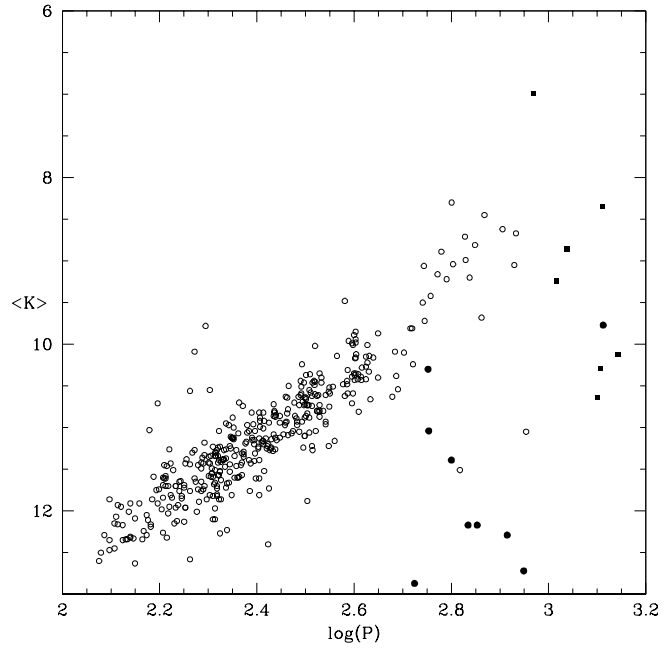

Fig. 3. The ($M_{\rm K}, \log P$) diagram for LPVs in the LMC. Symbols are as in Fig. 2

visible LPVs. This is just as expected from the evolutionary tracks of AGB stars during the high mass loss rate, superwind phase of evolution. The long periods are caused by the reduction in stellar mass (which directly increases the period through the period-mass-radius relation) and the reduction in stellar effective temperature and consequent increase in stellar radius that results from the decrease in envelope mass (Vassiliadis & Wood 1993).

The OH/IR stars near the Galactic Centre also demonstrate the evolution to long periods expected from theory (Jones et al 1994; Wood et al 1998; Blommaert et al 1998). However, because of the very large and variable reddening to the Galactic Centre region, the luminosities of the Galactic Centre sources are somewhat uncertain and direct comparison with theory is not as simple as in the case of the LMC.

The luminosities of the TRM sources are significantly fainter than those of the objects observed by Wood et al. (1992) (with the exception of the object in common, TRM 60). Comparison with the evolutionary tracks in Fig. 2 shows that the majority of the large amplitude TRM variables (6 out of 9 sources) have luminosities and periods consistent with them currently evolving on the very tip of the AGB occupied by stars of initial mass $\sim$1.5 $M_{\odot}$, corresponding to an age of 2-3$\times10^9$ years (Vassiliadis & Wood 1993). Studies of the star formation history of the LMC show that there was a large enhancement on the star formation rate $\sim$2-3 Gyr ago (Gallagher et al. 1996; Stappers et al. 1997). Thus, the low luminosity TRM sources seen here appear to come from the tip of the dominant AGB star population of the LMC.

4.2. The population of dust-enshrouded AGB stars in the LMC

Given that there is a large population of $\sim$2 Gyr old stars in the LMC, but that we know of only six dust-enshrouded AGB stars originating from this population, it is interesting to estimate how many other such objects might exist in the LMC. The lifetime for the superwind phase of AGB evolution is given roughly by the total envelope mass lost ($\sim$0.9 $M_{\odot}$ for the 1.5 $M_{\odot}$ stars) divided by the mass loss rate $\dot{M}$. An estimate of $\dot{M}$ for these stars can be obtained from $S25$ and $M_{\rm bol}$ using the formula for $\dot{M}_{25}$ given by Wood et al. (1992), assuming a wind expansion velocity of 11 km s^{-1} typical for LMC OH/IR stars (Wood et al. 1992). The mass loss rate $\dot{M}_{25}$ derived for the low luminosity TRM sources is 0.3-1$\times10^{-4} M_{\odot}$ yr^{-1}, and the duration of the superwind phase is then $\sim$1-3$\times10^4$ years. This is a typical planetary nebula lifetime, and since the dust-enshrouded AGB stars are the immediate precursors of planetary nebulae, the number of dust-enshrouded AGB stars in the LMC should be similar to the number of planetary nebulae, which is estimated to be $\sim$640 by Boroson & Liebert (1989). Thus the 15 dust-enshrouded, large

amplitude LPVs now known in the LMC (from this paper and Wood et al. 1992) probably represent only a few percent of the total population of such stars.

The difficulty of detecting LMC AGB stars in the superwind phase with IRAS has been known for a long time. For example, Frogel & Richer (1983) predicted that only AGB stars with $M_{\rm bol} < -6.5$ might be detected in standard observing mode. Nevertheless, the deep catalogs of Schwering (1988) and Reid et al. (1990) could contain many dust-enshrouded AGB stars. Indeed, the stars studied here are a sample selected from the Reid et al. (1990) catalog by Reid (1991). More recently, Loup et al. (1997) have selected a total of 198 obscured AGB candidates in the LMC from the catalogs of Schwering (1988) and Reid et al. (1990). Subsequent ground-based observations have greatly reduced this list to ∼46 plausible AGB candidates: 34 are listed in Table 7 of Zijlstra et al. (1996), and an additional 12 are given in Table 1 of van Loon et al. (1997). Fourteen of the 34 candidates in Zijlstra et al. have been shown here or by Wood et al. (1992) to be unambiguously AGB stars because of their long-period variability. There are almost certainly many hundreds of dust-enshrouded AGB stars as yet undetected in the LMC.

Another way to detect dust-enshrouded AGB stars in the LMC is to carry out a JHK survey. A start on such work has been made by Tanabé et al. (1997) who have detected a dusty AGB star near each of the rich, intermediate-age LMC clusters NGC1783 and NGC1978. The bolometric magnitudes derived for these objects by Tanabé et al. (1997) agree very well with the bolometric magnitudes of the six low luminosity, large amplitude TRM sources studied here. This result is consistent with both groups of stars belonging to a population of age a few Gyr.

It might be thought that the I surveys for LMC LPVs would provide yet another source of dust-enshrouded AGB stars. These surveys and subsequent JHK photometry have revealed a small number of objects with long periods ($\gtrsim$500 days) and low luminosities well below the normal, optically-visible LPV sequence in the ($M_{\rm bol}$, $\log P$) plane (e.g. Hughes & Wood 1990, see Fig. 2 in this paper; Reid et al. 1995). However, the published infrared colours of these objects ($0.45 \leq J-K \leq 2.67$) are consistent with them being essentially unreddened M or C stars, which have $0.8 \lesssim J-K \lesssim 3.1$ compared to $<J-K> > 3.9$ for the dust-enshrouded AGB stars in the present sample. It is most likely that these stars have had incorrect periods (which are too long) assigned to them.

4.3. Carbon or oxygen-rich shells?

The observations reported here do not reveal whether the large amplitude variables are carbon or oxygen-rich. However, there is some spectral information available in the literature for a few sources. As noted above, the three bright non-variable or small amplitude objects TRM 101, 108 and 129 are known M stars. The bright source TRM 60 was found by Wood et al (1992) to be an OH maser and it is therefore oxygen-rich. Zijlstra et al. (1996) obtained TIMMI observations of TRM 4 from which they tentatively assign an oxygen-rich status. However, confusion about the identity of IRAS sources can lead to incorrect classifications. For example, Reid et al. (1990) showed spectra of candidate stars for the sources TRM 72 and 88 (both candidates were C stars). In both cases, the stars for which spectra were obtained are not the variable stars found here, these variables almost certainly being the IRAS sources. Inspections of the infrared images obtained in this study show a bright star at the positions listed by Reid et al. for their observed stars: in addition, these stars are many magnitudes brighter at I than would be expected from the JHK photometry of the corresponding variable star. Groenewegen & Blommaert (1998) also show a C star spectrum for a TRM 88 candidate but it is not clear whether the star they observed is the variable star discussed here or the bright C star of Reid et al. (1990) ∼15″ to the south-east.

Zijlstra et al. (1996) and van Loon et al. (1998) show that for some $H-K$ ranges, carbon and M stars may be separated in the ($[K]-[12]$, $H-K$) plane. TRM 88 is designated a C star by van Loon et al. (1998) while TRM 4, 20 and 77 are designated as M stars. However, there is a large scatter about the C and M sequences and these assignmenst must be treated as very suspect. In summary then, apart from the previously known source TRM 60, the sources TRM 4, 20 and 77 have tentative identifications as oxygen-rich stars while TRM 88 is tentatively identified as a C star.

The three low luminosity stars designated as oxygen-rich have been shown above to be evolving off the intermediate-age AGB. Since intermediate-age LMC clusters generally have C stars at the tip of their optically-visible AGBs (Frogel et al. 1990), and since the dust-enshrouded AGB stars studied here should have evolved from these stars, it would be surprising if these stars are indeed oxygen-rich. Similarly, the majority of the optically-visible LPVs in the LMC with -4.5> $M_{\rm bol}$ > -5 (from which the dust-enshrouded stars should have evolved) are C stars, once again suggesting that the low luminosity, dust-enshrouded stars should be carbon-rich. A definite assignment of chemical type to these stars is badly needed.

4.4. The ($M_{\rm bol}, \log P$) and ($M_{\rm K}, \log P$) relations

Finally, it is worth commenting on the ($M_{\rm bol}, \log P$) and ($M_{\rm K}, \log P$) relations obeyed by dust-enshrouded LPVs (including OH/IR stars) as these might in principle be used for distance determination. For optically-visible LPVs in the LMC with periods $\lesssim$450 days, the above period-luminosity relations are certainly well-defined, with relative small scatter (Feast et al. 1989; Hughes & Wood 1990). There has been some suggestion that dust-enshrouded AGB stars with long periods may lie on an extension of the ($M_{\rm bol}, \log P$) relation for LPVs with $P \lesssim$450 days (Feast 1985; Whitelock et al. 1991; Whitelock 1995). However, the results in Fig. 2 show that this is not the case. The six large amplitude TRM sources with $M_{\rm bol} \gtrsim -5$ are much less luminous than expected from an extension of the sequence of optically-visible LPVs with $P \lesssim 450$ days: their positions in the ($M_{\rm bol}, \log P$) diagram are, however, just as predicted by the theoretical tracks of Vassiliadis & Wood (1993) – see Sect. 4.1.

A similar and more dramatic deviation of the dust-enshrouded LPVs from the optically-visible LPV sequence is shown in the ($M_{\rm K}, \log P$) diagram (Fig. 3). The shift in the spectral energy distribution to long wavelengths caused by dust makes the K magnitudes of dust-enshrouded stars much fainter than those of optically-visible stars of similar $M_{\rm bol}$.

5. Summary

Twelve LMC point sources with IRAS colours similar to those of AGB stars in the superwind phase of evolution have been monitored in the infrared for 1880 days. Nine of the candidates turn out to be pulsating, large amplitude, dust-enshrouded AGB stars. Periods from 530 to 1295 days have been determined for these objects. Six of the dust-enshrouded AGB stars come from the dominant population of intermediate-age stars in the LMC, with initial masses of $\sim$1.5 $M_{\odot}$ and ages of a few Gyr. It is argued that there should be $\sim$640 dust-enshrouded AGB stars in the LMC and that most of these are as yet undetected.

Since AGB stars at the optically-visible tips of intermediate-age clusters are generally C stars, it would be expected that the dust-enshrouded stars evolving from them would also be carbon-rich. However, tentative spectral classifications in the literature suggest that three of the dust-enshrouded AGB stars are oxygen-rich: this result needs verification.

The position of the objects in the ($M_{\rm bol}$, $\log P$) plane is consistent with that predicted by theoretical models of AGB stars in the superwind phase of evolution. However, the dust-enshrouded stars do not fall on extensions of the ($M_{\rm bol}$, $\log P$) or ($M_{\rm K}$, $\log P$) relations exhibited by optically-visible LPVs with periods $\lesssim$450 days.

References

Blommaert J.A.D.L., van der Veen W.E.C.J., Van Langevelde H.J., Habing H.J., Sjouwerman L.O. 1998, A&A 329, 991

Boroson T.A. & Liebert J., 1989, ApJ 339, 844

Feast M.W., 1985, in The Extragalactic Distance Scale, eds. S. van den Bergh & C.J. Pritchet, ASP Conf. Ser. 4, p.9

Feast M.W., Glass I.S., Whitelock P.A., Catchpole R.M., 1989, MNRAS 241, 375

Frogel J.A., Richer H.B., 1983, ApJ 275, 84

Frogel J.A., Mould J., Blanco V.M., 1990, ApJ 352, 96

Gallagher J.S., et al. 1996, ApJ 466, 742

Glass I.S., Reid, N., 1985, MNRAS 214, 405

Groenewegen M.A.T., Blommaert J.A.D.L., 1998, A&A 332, 25

Harvey P.M., Bechis K.P., Wilson W.J., Ball J.S., 1974, ApJS 27, 331

Hughes S.M.G., 1989, AJ 97, 1634

Hughes S.M.G., Wood P.R., 1990, AJ 99, 784

Jones T.J., McGregor P., Gehrz R.D., Lawrence G.F. 1994, AJ 107, 1111

Le Bertre T., 1993, A&AS 97, 729

Loup C., Zijlstra A.A., Waters L.B.F.M., Groenewegen M.A.T., 1997, A&A 125, 419

McGregor P.J., 1994, PASP 106, 508

McGregor P.J., Hyland A.R., 1981, ApJ 250, 116

McGregor P., Hart J., Hoadley D., Bloxham G., 1994, in Infrared Astronomy with Arrays, ed. I. McLean (Kluwer), p.299

Reid N., 1991, ApJ 382, 143

Reid N., Glass I.S., Catchpole R.M., 1988, MNRAS 232, 53

Reid N., Tinney C., Mould J., 1990, ApJ 348, 98

Reid I.N., Hughes S.M.G., Glass I.S., 1995, MNRAS 275, 331

Schwering P., 1988, An Infrared Study of the Magellanic Clouds, Thesis, Leiden University.

Stappers B.W., et al., 1997, PASP 109, 292

Stellingwerf R.F., 1978, ApJ, 224, 953

Tanabé T., Nishida S., Matsumoto S. et al., 1997, Nature 385, 509

Vassiliadis E., Wood P.R., 1993, ApJ 413, 641

van Loon J. Th., Zijlstra A., Whitelock P.A. et al., 1997, A&A 325, 585

van Loon J. Th., Zijlstra A., Whitelock P.A. et al., 1998, A&A 329, 169

Whitelock P., 1995, in Astrophysical Applications of Stellar Pulsation, eds. R.S. Stobie & P.A. Whitelock, ASP Conf. Ser. 83, p.165

Whitelock P., Feast M., Catchpole R., 1991, MNRAS 248, 276

Wood P.R., Bessell M.S., Fox, M.W., 1983, ApJ 272, 99

Wood P.R., Bessell M.S., Paltoglou, G., 1985, ApJ 290, 477

Wood P.R., Whiteoak J.B., Hughes S.M.G. et al., 1992, ApJ 397, 552

Wood P.R., Habing, H.J., McGregor, P.J., 1998, A&A, in press

Zijlstra A., Loup C., Waters L.B.F.M. et al., 1996, MNRAS 279, 32